TÉCNICO LISBOA

Thesis Title

Candidate Full Name

Thesis to obtain the Master of Science Degree in

Aerospace Engineering

Supervisor(s): Prof. Full Name 1
Dr. Full Name 2

Examination Committee

Chairperson: Prof. Full Name
Supervisor: Prof. Full Name 1 (or 2)
Member of the Committee: Prof. Full Name 3

Month Year

Dedicated to someone special...

Acknowledgments

A few words about the university, financial support, research advisor, dissertation readers, faculty or other professors, lab mates, other friends and family...

Resumo

Inserir o resumo em Português aqui com o máximo de 250 palavras e acompanhado de 4 a 6 palavras-chave...

Palavras-chave: palavra-chave1, palavra-chave2,...

Abstract

Due to their inherent non-linear dynamics, designing control systems for both rotary and fixed wing aircraft is a non-trivial task, where using linear control approaches often reveal to be inaccurate. Feedback linearization is an approach to non-linear control design that algebraically transforms a non-linear system onto a linear one. From the linearised system linear control techniques can be used. However this approach, as well as other state-of-the art control systems such as model predictive control, backstepping and gain scheduling require the *a priori* exact mathematical model of the system to be controlled [1]. The lack of such a model leads to errors in the calculation of the model inversion, necessary to implement feedback linearization. Indeed, while feedback linearization control shows good tracking, it has poor disturbance rejection, that ultimately lead to these inversion errors [2]. One solution to this problem that has gained momentum over the last years is the use augmentation algorithms, namely neural networks and other intelligent algorithms, to minimize and cancel this error[3], [4], [5]. This thesis therefore aims to discuss and implement the existing alternatives to augment the precision, robustness and overall performance of feedback linearization control.

Keywords: non-linear control, feedback linearization, neural network, flight control

Contents

List of Tables

List of Figures

Chapter 1

Introduction

Insert your chapter material here...

1.1 Motivation

Define: usefulness of NLI vs robust control and problems of NLI

1.2 Topic Overview

Brief description of the solutions to be studied and how they will be used to improve control

1.3 Objectives

Goals: create systems able to adapt to changes of the airplane's dynamic

1.4 Thesis Outline

Background includes in this order: NLI theory, NLI problematic, neural network theory Implementation: ? Results: ???

Chapter 2

Background

On this chapter the aircraft model used for this work will be described firstly. A theoretical model of the plane's dynamics will be discussed, and implementation detail will be provided on the chapter 3. The control strategy used will then follow, giving an overview of the feedback linearisation approach, as well as its limitations, namely its sensitivity to inversion errors and external interferences. An attempt to solve these limitation will be made, suggesting some solutions and finally describing the chosen methodology for this case.

2.1 Airplane Model

The work made in this thesis was built on top of the work done by H. Escamilla Nuñez and F. Mora Camino on 4D trajectory tracking [6]. The model used in this work of a six degree of freedom transport aircraft will be described in this section.

2.1.1 Frames of reference

The first step before describing the dynamics of a commercial aircraft will be to define the frames of reference used to do so. The first frame of reference, on which 4D trajectories are described, corresponds to the WGS84 frame of reference. A second frame of reference corresponding to the aircraft's body frame will be used to provide its fast rotational dynamics. Lastly all aerodynamic forces will be applied in the axial directions of the wind frame. This frame is aligned to the wind speed vector relative to the airplane, given by both the angle of attack α and the sideslip angle β. For these last two frames of reference, a rotation matrix can be defined from the wind frame to the body frame by

$$R_{WB} = \begin{bmatrix} c_\alpha c_\beta & -c_\alpha s_\beta & -s_\alpha \\ s_\beta & c_\beta & 0 \\ s_\alpha c_\beta & -s_\alpha s_\beta & c_\alpha \end{bmatrix} \tag{2.1}$$

To describe the attitude of the plane Euler angles will also be used, namely $\phi\{-\pi, \pi\}; \theta\{-\frac{\pi}{2}, \frac{\pi}{2}\}; \psi\{-\pi, \pi\}$.

From these angles the rotation matrix from the body to the earth's frame is given by

$$R_{BE} = \begin{bmatrix} c_\theta c_\psi & s_\phi s_\theta c_\psi - c_\phi s_\psi & c_\phi s_\theta c_\psi + s_\phi s_\psi \\ c_\theta c_\psi & s_\phi s_\theta s_\psi + c_\phi c_\psi & c_\phi s_\theta s_\psi - s_\phi c_\psi \\ -s_\theta & s_\phi c_\theta & c_\phi c_\theta \end{bmatrix} \tag{2.2}$$

2.1.2 Fast Dynamics

The considered actuators of the aircraft that control its attitude are given by $\delta = [\delta_{ail}\delta_{ele}\delta_{rud}]^T$, each applying a torque along an axis of the body frame. These torques are giver by

$$\begin{bmatrix} L' \\ M \\ N \end{bmatrix} = \frac{1}{2}\rho S V_a^2 \left(\begin{bmatrix} bC_l \\ \bar{c}C_m \\ bC_n \end{bmatrix} + C_\delta \delta \right) \tag{2.3}$$

where $\bar{c}$ and b represent the wing chord length and span respectively, C_δ and the moment coefficients $[C_l C_m C_n]^T$ are given by

$$C_\delta = \begin{bmatrix} bC_{l\delta_{ail}} & 0 & bC_{l\delta_{rud}} \\ 0 & \bar{c}C_{m\delta_{ele}} & 0 \\ bC_{n\delta_{ail}} & 0 & bC_{n\delta_{rud}} \end{bmatrix} \tag{2.4}$$

$$\begin{bmatrix} C_l \\ C_m \\ C_n \end{bmatrix} = \begin{bmatrix} C_{l\beta}\beta + C_{l_p} p\frac{b}{2V_a} + C_{l_r} r\frac{b}{2V_a} \\ C_{m_0} + C_{m_\alpha}\alpha + C_{m_q} q\frac{\bar{c}}{2V_a} \\ C_{n\beta}\beta + C_{n_p} p\frac{b}{2V_a} + C_{n_r} r\frac{b}{2V_a} \end{bmatrix} \tag{2.5}$$

Where p, q, r are the body's angular rates ($\Omega = [pqr]^T$) and V_a is the airspeed. The method of obtaining of the coefficients of equation 2.5 will be provided in the chapter to follow. Having defined the torques applied to the aircraft the rotational dynamics equation can now be stated as per [6], I being the aircraft's inertial matrix.

$$\dot{\Omega} = I^{-1} M_{ext} - I^{-1}\Omega \times (I\Omega) \tag{2.6a}$$

$$\dot{\Omega} = \frac{1}{2}\rho S I^{-1} V_a^2 \left(\begin{bmatrix} bC_l \\ \bar{c}C_m \\ bC_n \end{bmatrix} + C_\delta \delta \right) - I^{-1}\Omega \times (I\Omega) \tag{2.6b}$$

These two equations can be rearranged to account for the effect of the wind, allowing further on to simulate the behaviour of the airplane in the presence of wind disturbances. Let $\vec{V_G} = [u \quad v \quad w]^T$ be the speed of the CG relative to the ground, $\vec{V}$ the speed of the CG relative to the air mass and $\vec{W}$ the

speed of the wind relative to the ground, then as per Etkin and Reid [**?**]

$$\vec{V_G} = \vec{V} + \vec{W} = \begin{bmatrix} V_a c_\alpha c_\beta + V_{w_x} \\ V_a s_\beta + V_{w_y} \\ V_a s_\alpha c_\beta + V_{w_z} \end{bmatrix} \tag{2.7}$$

and α and β can be computed by

$$\alpha = arctan\left(\frac{w}{u}\right) \tag{2.8a}$$

$$\beta = arctan\left(\frac{v}{V_a}\right) \tag{2.8b}$$

From these three equations, differentiating 2.8a and 2.8b comes that

$$\begin{bmatrix} \dot{\alpha} \\ \dot{\beta} \end{bmatrix} = \begin{bmatrix} H_{11} & 1 & H_{13} \\ H_{21} & 0 & H_{23} \end{bmatrix} \begin{bmatrix} p \\ q \\ r \end{bmatrix} + \begin{bmatrix} Q_1 \\ Q_2 \end{bmatrix} \tag{2.9}$$

SEE ANNEX HERE

The angular rates are also related to the Euler angles. The relationship between the euler angles and the rotation rates is also one that will prove useful when implementing the model on a Matlab simulation, and is given by

$$\begin{bmatrix} \dot{\phi} \\ \dot{\theta} \\ \dot{psi} \end{bmatrix} = \begin{bmatrix} 1 & tg_\theta s_\phi & tg_\theta c_\phi \\ 0 & c_\phi & -s_\phi \\ 0 & \frac{s_\phi}{c_\theta} & \frac{c_\phi}{c_\theta} \end{bmatrix} \begin{bmatrix} p \\ q \\ r \end{bmatrix} \tag{2.10}$$

2.2 Guidance Dynamics

This subsection on the forces applied to aircraft, introducing a new actuation variable, the thrust force T. These forces are applied along the three axis of the wind frame, lift, drag and side force, given by

$$\begin{bmatrix} D \\ Y \\ L \end{bmatrix} = \frac{1}{2}\rho S V_a^2 \begin{bmatrix} C_D \\ C_Y \\ C_L \end{bmatrix} \tag{2.11}$$

Once again, the method used to compute these coefficients will be given in the chapter 3 in detail. These coefficients, similarly to the moment coefficient, are functions of the angle of attack, sideslip angle and airspeed, the three most relevant variables when determining aerodynamic forces and moments. Although aerodynamic forces are usually expressed on the wind frame, as the thrust is always applied along the x axis of the body frame, it is necessary to rotate the aerodynamic forces to this frame. This way the sum of the airplane's forces can be obtained.

$$\begin{bmatrix} F_{xa} \\ F_{ya} \\ F_{za} \end{bmatrix} = R_{WB} \begin{bmatrix} -D \\ Y \\ -L \end{bmatrix} \tag{2.12}$$

From Newton's Second Law comes the aircraft's acceleration

$$\begin{bmatrix} \dot{u} \\ \dot{v} \\ \dot{w} \end{bmatrix} = \begin{bmatrix} \frac{1}{m}(F_{xa} + T) - gs_\theta + rv - qw \\ \frac{1}{m}F_{ya} + gc_\theta s_\phi + pw - ru \\ \frac{1}{m}F_{za} + gc_\theta c_\phi + qu - pv \end{bmatrix} \tag{2.13}$$

An expression in the Earth frame can also be obtained

$$\begin{bmatrix} \ddot{x_E} \\ \ddot{y_E} \\ \ddot{z_E} \end{bmatrix} = \frac{1}{m} R_{BE} \begin{bmatrix} F_{xa} + T \\ F_{ya} \\ F_{za} \end{bmatrix} + \begin{bmatrix} 0 \\ 0 \\ g \end{bmatrix} \tag{2.14}$$

2.2.1 Actuator Dynamics

Finally, to simulate the delay response in actuation in order to have a realistic simulation, first order systems were introduced to the actuator dynamics as per [6]. For the control surfaces δ_i, given a desired δ_i^d comes

$$\dot{\delta}_i = \frac{1}{\xi_i}(\delta_i^d - \delta_i) \tag{2.15}$$

Similarly for the thrust

$$\dot{T} = \frac{1}{\xi_T}(T^d - T) \tag{2.16}$$

ξ_i and ξ_T being time constants. As the responsiveness of the resultant thrust will be much slower than that of the control surfaces, $\xi_T >> \xi_i$

2.3 Feedback linearisation

Feedback linearisation, also known as dynamic inversion, is an approach based on the idea of algebraically transforming a non-linear system into a linear one, from which linear control laws can be used to control the resulting system. Unlike Jacobian linearisation, that assumes linearity of the system around an equilibrium value, feedback linearisation implements a feedback loop that cancels non-linearities of the given system.

2.4 Limitations of feedback linearisation

2.4.1 Control improvement

2.5 Neural Networks

Chapter 3

Implementation

Insert your chapter material here...

3.1 Numerical Model

Description of the numerical implementation of the models explained in Chapter 2...

3.2 Verification and Validation

Basic test cases to compare the implemented model against other numerical tools (verification) and experimental data (validation)...

Chapter 4

Results

Insert your chapter material here...

4.1 Problem Description

Description of the baseline problem...

4.2 Baseline Solution

Analysis of the baseline solution...

4.3 Enhanced Solution

Quest for the optimal solution...

4.3.1 Figures

Insert your section material and possibly a few figures...

Make sure all figures presented are referenced in the text!

Images

Figure 4.1: Caption for figure.

(a) Airbus A320

(b) Bombardier CRJ200

Figure 4.2: Some aircrafts.

Make reference to Figures 4.1 and 4.2.

By default, the supported file types are *.png,.pdf,.jpg,.mps,.jpeg,.PNG,.PDF,.JPG,.JPEG*.

See `http://mactex-wiki.tug.org/wiki/index.php/Graphics_inclusion` for adding support to other extensions.

Drawings

Insert your subsection material and for instance a few drawings...

The schematic illustrated in Fig. 4.3 can represent some sort of algorithm.

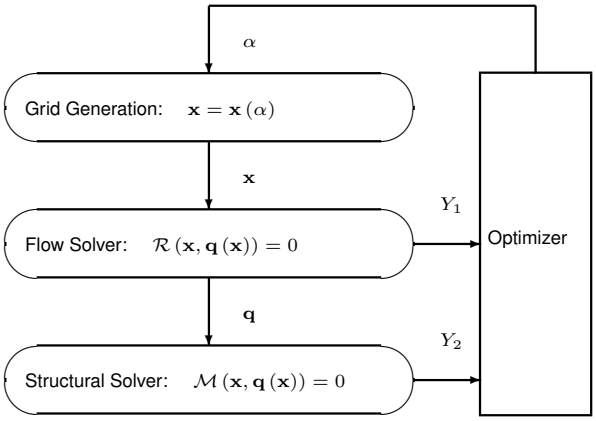

Figure 4.3: Schematic of some algorithm.

4.3.2 Equations

Equations can be inserted in different ways.

The simplest way is in a separate line like this

$$\frac{\mathrm{d}q_{ijk}}{\mathrm{d}t} + \mathcal{R}_{ijk}(\mathbf{q}) = 0\,. \tag{4.1}$$

If the equation is to be embedded in the text. One can do it like this $\partial\mathcal{R}/\partial\mathbf{q} = 0$.

It may also be split in different lines like this

$$\begin{aligned} \text{Minimize} \quad & Y(\alpha, \mathbf{q}(\alpha)) \\ \text{w.r.t.} \quad & \alpha\,, \\ \text{subject to} \quad & \mathcal{R}(\alpha, \mathbf{q}(\alpha)) = 0 \\ & C(\alpha, \mathbf{q}(\alpha)) = 0\,. \end{aligned} \tag{4.2}$$

It is also possible to use subequations. Equations 4.3a, 4.3b and 4.3c form the Naver–Stokes equations 4.3.

$$\frac{\partial \rho}{\partial t} + \frac{\partial}{\partial x_j}\left(\rho u_j\right) = 0\,, \tag{4.3a}$$

$$\frac{\partial}{\partial t}\left(\rho u_i\right) + \frac{\partial}{\partial x_j}\left(\rho u_i u_j + p\delta_{ij} - \tau_{ji}\right) = 0, \quad i = 1, 2, 3\,, \tag{4.3b}$$

$$\frac{\partial}{\partial t}\left(\rho E\right) + \frac{\partial}{\partial x_j}\left(\rho E u_j + p u_j - u_i \tau_{ij} + q_j\right) = 0\,. \tag{4.3c}$$

4.3.3 Tables

Insert your subsection material and for instance a few tables...

Make sure all tables presented are referenced in the text!

Follow some guidelines when making tables:

- Avoid vertical lines
- Avoid “boxing up” cells, usually 3 horizontal lines are enough: above, below, and after heading
- Avoid double horizontal lines
- Add enough space between rows

Model	C_L	C_D	C_{My}
Euler	0.083	0.021	-0.110
Navier–Stokes	0.078	0.023	-0.101

Table 4.1: Table caption.

Make reference to Table 4.1.

Tables 4.2 and 4.3 are examples of tables with merging columns:

An example with merging rows can be seen in Tab.4.4.

If the table has too many columns, it can be scaled to fit the text widht, as in Tab.4.5.

	Virtual memory [MB]	
	Euler	Navier–Stokes
Wing only	1,000	2,000
Aircraft	5,000	10,000
(ratio)	$5.0\times$	$5.0\times$

Table 4.2: Memory usage comparison (in MB).

	$w = 2$			$w = 4$		
	$t = 0$	$t = 1$	$t = 2$	$t = 0$	$t = 1$	$t = 2$
$dir = 1$						
c	0.07	0.16	0.29	0.36	0.71	3.18
c	-0.86	50.04	5.93	-9.07	29.09	46.21
c	14.27	-50.96	-14.27	12.22	-63.54	-381.09
$dir = 0$						
c	0.03	1.24	0.21	0.35	-0.27	2.14
c	-17.90	-37.11	8.85	-30.73	-9.59	-3.00
c	105.55	23.11	-94.73	100.24	41.27	-25.73

Table 4.3: Another table caption.

ABC	header			
	1.1	2.2	3.3	4.4
IJK	group		0.5	0.6
			0.7	1.2

Table 4.4: Yet another table caption.

Variable	a	b	c	d	e	f	g	h	i	j
Test 1	10,000	20,000	30,000	40,000	50,000	60,000	70,000	80,000	90,000	100,000
Test 2	20,000	40,000	60,000	80,000	100,000	120,000	140,000	160,000	180,000	200,000

Table 4.5: Very wide table.

4.3.4 Mixing

If necessary, a figure and a table can be put side-by-side as in Fig.4.4

Legend		
A	B	C
0	0	0
0	1	0
1	0	0
1	1	1

Figure 4.4: Figure and table side-by-side.

Chapter 5

Conclusions

Insert your chapter material here...

5.1 Achievements

The major achievements of the present work...

5.2 Future Work

A few ideas for future work...

Bibliography

[1] S. et al. State-of-the-art intelligent flight control systems in unmanned aerial vehicles. *IEEE TRANSACTIONS ON AUTOMATION SCIENCE AND ENGINEERING*, 2017.

[2] A. Zulu and S. John. A review of control algorithms for autonomous quadrotors. *Open Journal of Applied Sciences*, 2014.

[3] A. K. S. et al. Neuro-adaptive augmented dynamic inversion controller for quadrotor. *IFAQ Papers Online*, 2016.

[4] M. P. et al. Augmentation of a non linear dynamic inversion scheme within the nasa ifcs f-15 wvu simulator. *Proceedings of the American Control Conference*, 2013.

[5] T. X. et al. Adaptive flight control for quadrotor uavs with dynamic inversion and neural networks. *IEEE Intemational Conference on Multisensor Fusion and Integration for Intelligent Systems (MFI)*, 2016.

[6] F. M. C. H. Escamilla Nuñez. Towards 4d trajectory tracking for transport aircraft. *IFAQ World Congress*, 2017.

Appendix A

Vector calculus

In case an appendix if deemed necessary, the document cannot exceed a total of 100 pages...

Some definitions and vector identities are listed in the section below.

A.1 Vector identities

$$\nabla \times (\nabla \phi) = 0 \tag{A.1}$$

$$\nabla \cdot (\nabla \times \mathbf{u}) = 0 \tag{A.2}$$

Appendix B

Technical Datasheets

It is possible to add PDF files to the document, such as technical sheets of some equipment used in the work.

B.1 Some Datasheet

SUNPOWER

C60 SOLAR CELL

MONO CRYSTALLINE SILICON

BENEFITS

Maximum Light Capture
SunPower's all-back contact cell design moves gridlines to the back of the cell, leaving the entire front surface exposed to sunlight, enabling up to 10% more sunlight capture than conventional cells.

Superior Temperature Performance
Due to lower temperature coefficients and lower normal cell operating temperatures, our cells generate more energy at higher temperatures compared to standard c-Si solar cells.

No Light-Induced Degradation
SunPower n-type solar cells don't lose 3% of their initial power once exposed to sunlight as they are not subject to light-induced degradation like conventional p-type c-Si cells.

Broad Spectral Response
SunPower cells capture more light from the blue and infrared parts of the spectrum, enabling higher performance in overcast and low-light conditions.

Broad Range Of Application
SunPower cells provide reliable performance in a broad range of applications for years to come.

The SunPower™ C60 solar cell with proprietary Maxeon™ cell technology delivers today's highest efficiency and performance.

The anti-reflective coating and the reduced voltage-temperature coefficients provide outstanding energy delivery per peak power watt. Our innovative all-back contact design moves gridlines to the back of the cell, which not only generates more power, but also presents a more attractive cell design compared to conventional cells.

SunPower's High Efficiency Advantage

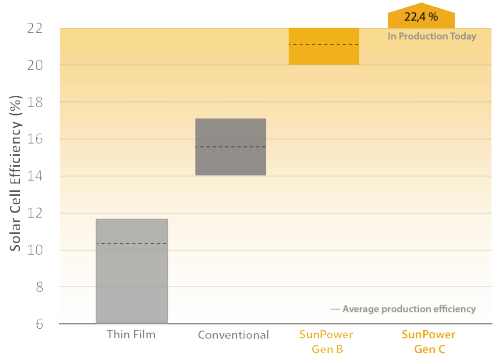

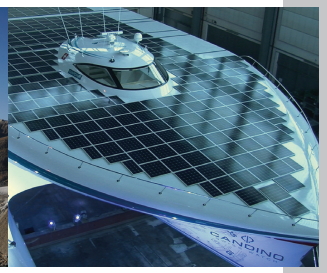

C60 SOLAR CELL

SUNPOWER

C60 SOLAR CELL

MONO CRYSTALLINE SILICON

Electrical Characteristics of Typical Cell at Standard Test Conditions (STC)

STC: 1000W/m², AM 1.5g and cell temp 25°C

Bin	Pmpp (Wp)	Eff. (%)	Vmpp (V)	Impp (A)	Voc (V)	Isc (A)
G	3.34	21.8	0.574	5.83	0.682	6.24
H	3.38	22.1	0.577	5.87	0.684	6.26
I	3.40	22.3	0.581	5.90	0.686	6.27
J	3.42	22.5	0.582	5.93	0.687	6.28

All Electrical Characteristics parameters are nominal
Unlaminated Cell Temperature Coefficients
Voltage: -1.8 mV / °C Power: -0.32% / °C

Positive Electrical Ground

Modules and systems produced using these cells must be configured as "positive ground systems".

TYPICAL I-V CURVE

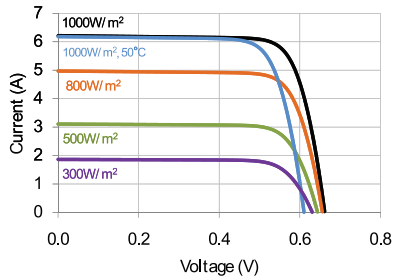

SPECTRAL RESPONSE

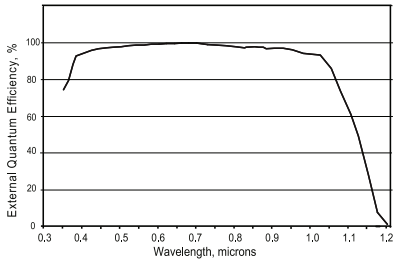

Physical Characteristics

Construction:	All back contact
Dimensions:	125mm x 125mm (nominal)
Thickness:	165µm ± 40µm
Diameter:	160mm (nominal)

Cell and Bond Pad Dimensions

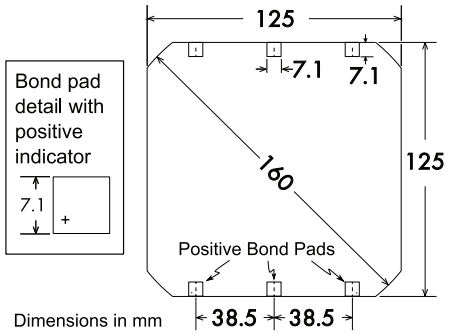

Bond pad area dimensions are 7.1mm x 7.1mm
Positive pole bond pad side has "+" indicator on leftmost and rightmost bond pads.

Interconnect Tab and Process Recommendations

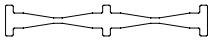

Tin plated copper interconnect. Compatible with lead free process.

Packaging

Cells are packed in boxes of 1,200 each; grouped in shrink-wrapped stacks of 150 with interleaving. Twelve boxes are packed in a water-resistant "Master Carton" containing 14,400 cells suitable for air transport.

Interconnect tabs are packaged in boxes of 1,200 each.

About SunPower

SunPower designs, manufactures, and delivers high-performance solar electric technology worldwide. Our high-efficiency solar cells generate up to 50 percent more power than conventional solar cells. Our high-performance solar panels, roof tiles, and trackers deliver significantly more energy than competing systems.

sunpowercorp.com

Document #001-66352 Rev** A4_en